BAEYER-VILLIGER OXIDATION OVER Sn(IV) PHOSPHONATES

A Senior Scholars Thesis

by

SANDANI SAMARAJEEWA

Submitted to the Office of Undergraduate Research
Texas A&M University
in partial fulfillment of the requirements for the designation as

UNDERGRADUATE RESEARCH SCHOLAR

April 2008

Major: Chemistry

BAEYER-VILLIGER OXIDATION OVER Sn(IV) PHOSPHOANTES

A Senior Scholars Thesis

by

SANDANI SAMARAJEEWA

Submitted to the Office of Undergraduate Research
Texas A&M University
in partial fulfillment of the requirements for the designation as

UNDERGRADUATE RESEARCH SCHOLAR

Approved by:

Research Advisor: Abraham Clearfield
Associate Dean for Undergraduate Research: Robert C. Webb

April 2008

Major: Chemistry

ABSTRACT

Baeyer-Villiger Oxidation over Sn(IV) Phosphonates

(April 2008)

Sandani Samarajeewa
Department of Chemistry
Texas A&M University

Research Advisor: Dr. Abraham Clearfield
Department of Chemistry

Baeyer-Villiger (BV) oxidations are used to convert ketones and aldehydes to esters and phenols. These ester and phenols are useful building blocks in designing more complex organic materials in pharmaceutical chemistry. By using catalysts in the BV oxidations, high selectivity and conversion can be obtained while the waste production can be minimized. We have synthesized a new family of layered Sn(IV) phosphonate materials which are efficient catalysts in the BV oxidation of aromatic aldehydes. The most attractive feature of these catalysts is that the reaction can be carried out under solvent-free conditions using aqueous H_2O_2 (30 %) as the oxidant. Various Sn(IV) phosphonates have been synthesized using phosphonic acid in different solvent systems following a hydrothermal procedure. These catalysts have been characterized using X-Ray Powder Diffraction, Thermo Gravimetric Analysis and Surface Area and Pore Size Analysis. Following their synthesis, the catalytic ability of each of the samples was tested toward the BV oxidation of para substituted aromatic aldehydes to phenols. The products were

identified using Mass Spectroscopy and the percent conversion and selectivity of the reaction were measured using Gas Chromatography. A noticeable trend was found between percent conversion and high external surface area.

DEDICATION

I dedicate this to my father Upali Samarajeewa and mother Daya Samarajeewa for the invaluable encouragement they have given me to pursue my education in chemistry.

ACKNOWLEDGMENTS

I would like to thank my research adviser Dr. Abraham Clearfield for giving me the opportunity to conduct research in his lab, for his valuable advice and support extended during my undergraduate studies. I would also like to extend my gratitude to Dr. Sharath Kirumakki, the postdoctoral researcher whom I conducted research under for the past two years. Without his guidance I would have not been able to complete my research work successfully.

This study was supported by the National Science Foundation (NSF) through Grant DMR-0332453 and the Robert A. Welch Foundation Grant 0673A, for which grateful acknowledgment is made. The TAMU Microscopy & Imaging Center (MIC) facility is also acknowledged.

NOMENCLATURE

BV	Baeyer-Villiger
SEM	Scanning Electron Microscope
XRD	X-Ray Diffraction
TGA	Thermo Gravimetric Analysis
NMR	Nuclear Magnetic Resonance
H	Hydrogen
O	Oxygen
H_2O	Water
EtOH	Ethanol
H_2O_2	Hydrogen Peroxide
Sn	Tin
Å	Angstroms
DMSO	Dimethyl Sulfoxide
Ph	Phenyl
P	Phosphorus
SnPP	Tin Phenyl Phosphonate
SeO_2	Selenium Dioxide
HF	Hydrogen Fluoride
mL	Milliliters
mmol	Millimoles

°C	Celsius
Min	Minutes
H_3PO_3	Phosphorous Acid
θ	Theta Angle
BET	Brunauer-Emmett-Teller
K	Kelvins
GC	Gas Chromatography
MS	Mass Spectroscopy
FID	Flame Ionization Detector
mm	Millimeters
m	Meters
N_2	Nitrogen Gas
Cl	Chlorine
cc	Cubic Centimeters

TABLE OF CONTENTS

LIST OF FIGURES

FIGURE Page

FIGURE Page

LIST OF TABLES

CHAPTER I

INTRODUCTION

Baeyer-Villiger (BV) oxidation is named after the 1905 recipient of the Nobel Prize in Chemistry, German chemist Johann Friedrich Wilhelm Adolf von Baeyer and the Swiss chemist Victor Villiger.[1] The BV oxidation is the oxidative cleavage of a carbon-carbon bond adjacent to a carbonyl, which converts ketones to esters and aldehydes to phenols as shown in Scheme 1.

Scheme 1. Baeyer-Villiger oxidation of an aromatic aldehydes.

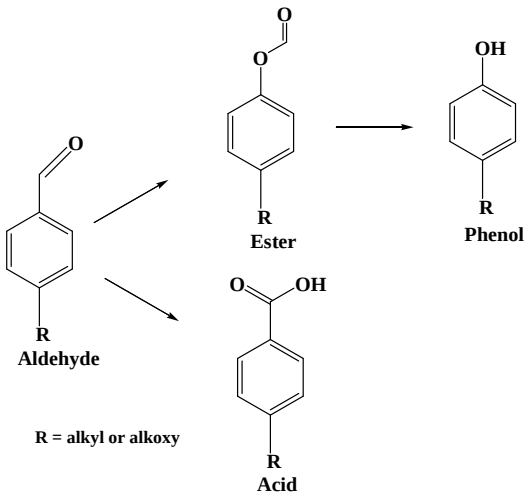

This thesis follows the style of *Journal of the American Chemical Society*.

These esters and phenols are useful building blocks in designing more complex organic materials in pharmaceutical chemistry. The conventional BV oxidation involves the use of an organic peracid. The main drawback of this procedure is that the organic peracid is expensive, hazardous and ecologically unattractive as it produces carboxylic acid salts as the by product.[2] The use of hydrogen peroxide is a "green" process, as water is the by product of this oxidation.

The main challenges to the BV oxidation are the compatibility of the solvent with aqueous H_2O_2 and finding the right catalyst which would activate the peroxide in the presence of water. There are a number of reports on the oxidation of cyclic ketones[3-6] using hydrogen peroxide but only a few on the oxidation of aromatic aldehydes, mainly because of the poor reactivity of the aromatic aldehydes. Homogenous catalysts such as SeO_2 and arylseleninic acids have been found to be efficient in the oxidation of aromatic aldehydes using aqueous hydrogen peroxide.[7] Corma and his group have designed Sn-beta zeolite and Sn-MCM-41 heterogeneous catalysts for the reaction of aromatic aldehydes with hydrogen peroxide in non-halogenated solvents such as dimethylformamide and dioxane.[8-11] They suggest that the catalyst activates the carbonyl compound and not the hydrogen peroxide, and this carbonyl activation makes these catalysts more selective.

We have developed a family of porous Sn(IV) phenylphosphonates that are layered materials, possess high surface area and with pore diameters in the 10-20 Å range.[12,13] The idealized structure of the Sn(IV) phenyl phosphonate is shown in Figure 1.

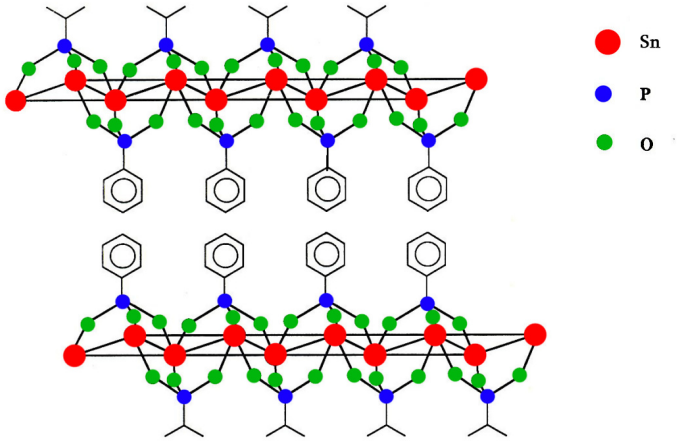

Figure 1. Idealized structure of Sn(IV) phenyl phosphonate.

In our research, the layered Sn(IV) phenyl phosphonates have been used as catalysts in the BV reaction and are found to be extremely active in the oxidation of aromatic aldehydes using 30% aqueous H_2O_2 solution. The most fascinating part of these catalysts is that the reaction proceeds more efficiently in the absence of any organic solvents.

In this study a series of catalysts were synthesized using different phosphonic acids and solvents. The structures of the catalysts were characterized using thermo gravimetric analysis, x-ray diffraction and surface area and pore size analysis. The Scanning Electron Microscopy (SEM) images of these samples showed that the tin phosphonate catalysts synthesized in the presence of ethanol tend to form nanoparticles which aggregate to form porous globules, whereas in the catalysts synthesized using water or dimethyl sulfoxide (DMSO) as solvents the particles were much bigger and better defined (Figure 2).

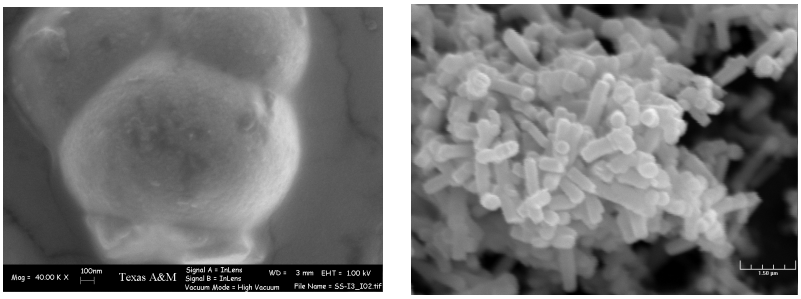

A) ethanol as solvent B) water or DMSO as solvent

Figure 2. SEM images of Sn phosphonates synthesized in different solvents.

To investigate the different effects of the catalysts on the conversion and selectivity of the BV oxidation, the reaction was carried out under varying reaction conditions. Different aromatic aldehydes, reaction times, temperatures, catalysts and catalyst weights were used to study the the catalytic activity. The conversion and selectivity of the reaction were calculated using gas chromatography and the products were identified using mass spectroscopy.

CHAPTER II

METHODS

We have prepared a series of catalysts in different solvents H_2O, EtOH, DMSO and mixed solvent systems with different phosphonic acids in between the layers. After the catalysts were characterized, they were used in the Baeyer-Villiger Oxidation of aromatic aldehydes. The influence of different solvent systems on the BV oxidation of different para substituted aldehydes was studied.

Synthesis of Sn(IV) phosphonates

$Sn(IV)(PhPO_3)_2$; H_2O, with HF

1.039 g of $SnCl_4.5H_2O$ (~3 mmol) was placed into a plastic beaker. DI water (10 mL) and HF (0.3 mL of 50% HF) were then added. In a separate beaker, 0.9435 g of $PhPO_3H_2$ (~6 mmol) was dissolved in DI water (10 mL). Once the ligand was dissolved, the two solutions were combined, leading to the immediate formation of a white suspension/gel. The mixture was then sealed and heated at 140 °C in a 40 mL Teflon liner for 3 days. The resulting white powder was filtered off and washed with ethanol and water. It was then dried at 60 °C overnight.

$Sn(IV)(PhPO_3)_2$; EtOH, with HF

1.0454 g of $SnCl_4.5H_2O$ (~3 mmol) was placed into a plastic beaker. Ethanol (10 mL) and HF (0.3 mL of 50% HF) were then added and mixed for 5 min. In a separate beaker, 0.9532 g of $PhPO_3H_2$ (~6 mmol) was dissolved in ethanol (10 mL). Once the ligand was

dissolved, the two solutions were combined, leading to the immediate formation of a clear solution. The mixture was then sealed and heated at 140 °C in a 40 mL Teflon liner for 3 days. The resulting white powder was filtered off and washed with ethanol and water. It was then dried at 60°C overnight.

$Sn(IV)(PhPO_3)_2$; DMSO, with HF

1.0459 g of $SnCl_4.5H_2O$ (~3 mmol) was placed into a plastic beaker. DMSO (10 mL) and HF (0.3 mL of 50% HF) were then added and mixed for 5 min. In a separate beaker, 0.9542 g of $PhPO_3H_2$ (~6 mmol) was dissolved in DMSO (10 mL). Once the ligand was dissolved, the two solutions were combined, leading to the immediate formation of a clear solution. The mixture was then sealed and heated at 140 °C in a 40 mL Teflon liner for 3 days. The resulting white powder was filtered off and washed with ethanol and water. It was then dried at 60 °C overnight.

$Sn(IV)Ph_2P_2$- HP; without HF; in DMSO and H_2O

0.3306 g of $SnCl_4.5H_2O$ (~1 mmol) was placed into a beaker containing DI water (10 mL) and mixed for 5 min. In a separate beaker, 0.3005 g 0f Ph_2P_2 (~1 mmol) and 0.078 g of H_3PO_3 (~1 mmol) were dissolved in DMSO (10 mL). Once the ligand was dissolved, the two solutions were combined and mixed (30 min). The mixture was then sealed and heated at 140 °C in a 40 mL Teflon liner for 3 days. The resulting white powder was filtered off and washed with ethanol and water. It was then dried at 60 °C overnight.

Sn(IV)Ph_2P_2- HP; with HF; in DMSO and H_2O

0.3405 g of $SnCl_4.5H_2O$ (~1 mmol) was placed into a plastic beaker. DI water (10 mL) and HF (0.1 mL) were then added and mixed for 5 min. In a separate beaker, 0.3014 g of Ph_2P_2 (~1 mmol) and 0.0781 g of H_3PO_3 (~1 mmol) were dissolved in DMSO (10 mL). Once the ligand was dissolved, the two solutions were combined and mixed (30 min). The mixture was then sealed and heated at 140°C in a 40 mL Teflon liner for 3 days. The resulting white powder was filtered off and washed with ethanol and water. It was then dried at 60 °C overnight.

Synthesis of mixed Sn(IV) phosphonates

$SnCl_4.5H_2O$: $PhPO_3H_2$: H_3PO_3 (3:4:2) – with HF; in DMSO and H_2O

1.039 g of $SnCl_4.5H_2O$ (~3 mmol) was placed into a plastic beaker. DI water (10 mL) and HF (2.4 mL of 48% wt) were then added and mixed for 5 min. In a separate beaker, 0.629 g of $PhPO_3H_2$ (~4 mmol) and 0.1632 g of H_3PO_3 (~2 mmol) were dissolved in DMSO (10 mL). Once the ligand was dissolved, the two solutions were combined and mixed (30 min). The mixture was then sealed and heated at 140°C in a 40 mL Teflon liner for 3 days. The resulting white powder was filtered off and washed with ethanol and water. It was then dried at 60°C overnight.

$SnCl_4.5H_2O$: $PhPO_3H_2$: H_3PO_3 (3:4:2) – without HF; in DMSO and H_2O

1.039 g of $SnCl_4.5H_2O$ (~3 mmol) was placed into a beaker containing DI water (10 mL) and mixed for 5 min. In a separate beaker, 0.629 g of $PhPO_3H_2$ (~4 mmol) and 0.1632 g

of H_3PO_3 (~2 mmol) were dissolved in DMSO (10 mL). Once the ligand was dissolved, the two solutions were combined and mixed (30 min). The mixture was then sealed and heated at 140 °C in a 40 mL Teflon liner for 3 days. The resulting white powder was filtered off and washed with ethanol and water. It was then dried at 60 °C overnight.

$SnCl_4.5H_2O$: $PhPO_3H_2$: H_3PO_3 (1:1:1) – with HF; in DMSO and H_2O

1.039 g of $SnCl_4.5H_2O$ (~3 mmol) was placed into a plastic beaker. DI water (10 mL) and HF (2.4 mL of 48 Wt%) were then added and mixed for 5 min. In a separate beaker, 0.4718 g of $PhPO_3H_2$ (~3 mmol) and 0.2448 g of H_3PO_3 (~3 mmol) were dissolved in DMSO (10 mL). Once the ligand was dissolved, the two solutions were combined and mixed (30 min). The mixture was then sealed and heated at 140 °C in a 40 mL Teflon liner for 3 days. The resulting white powder was filtered off and washed with ethanol and water. It was then dried at 60 °C overnight.

$SnCl_4.5H_2O$: $PhPO_3H_2$: H_3PO_3 (1:1:1) – without HF; in DMSO and H_2O

1.039 g of $SnCl_4.5H_2O$ (~3 mmol) was placed into a beaker containing DI water (10 mL) and mixed for 5 min. In a separate beaker, 0.4718 g of $PhPO_3H_2$ (~3 mmol) and 0.2448 g of H_3PO_3 (~3 mmol) were dissolved in DMSO (10 mL). Once the ligand was dissolved, the two solutions were combined and mixed (30 min). The mixture was then sealed and heated at 140°C in a 40 mL Teflon liner for 3 days. The resulting white powder was filtered off and washed with ethanol and water. It was then dried at 60°C overnight.

Catalyst characterization

X-Ray Diffraction

X-ray diffraction (XRD) patterns were obtained with a Bruker D 8 diffractometer, using Cu $K\ \alpha$ radiation (1.5406 Å) at 40 kV and 40 mA and a diffracted beam graphite monochromator. The measurements were recorded in steps of 0.04° with a count time of 1 s in the 2θ range of 2°–60°.

Surface Area and Pore Size Measurements

The BET surface area of the samples was determined from multipoint BET isotherms (Quantachrome Autosorb-1) using nitrogen as adsorbate at 77 K. Before the measurement, the samples were degassed at 225 °C for 12 h.

Thermo Gravimetric Analysis

Thermogravimetric analyses (TGA) were performed on a TA Instruments TGA Q-500 at a heating rate of 10 °C/min under air.

Baeyer-Villiger reaction

Experimental

In a typical reaction para-substituted aromatic aldehyde (3.7 mmol) was mixed with 0.9 mL of H_2O_2 and 0.025 g of catalyst. The solution was refluxed in a heated oil bath. Studies were carried out at varying temperatures, varying periods of reaction time and different amounts of catalysts to find the optimum reaction conditions. After the

completion of the reaction, the solution was cooled to room temperature and the catalyst was removed by gravity filtration. The reaction mixture was analyzed by GC to determine percent conversion of starting material and selectivity of the catalyst.

Characterization

The products were analyzed using an Agilent 6890 N_2 gas chromatograph (FID detector, column: HP-5, 30m x 5mm x 0.25 µm) and the products were confirmed by GC-MS.

CHAPTER III

RESULTS

The synthesized Sn(IV) phenylphosphonates were characterized using XRD, Surface Area and Pore Size Analysis and TGA. The first sharp peak on the XRD patterns corresponds to the interlayer d spacing of the layered SnPP materials. The XRD pattern of each catalyst is used to determine the layered structure of the material and to study the relationship between the interlayer d spacing and the catalytic ability of the SnPP. Surface area and pore size are important characteristics that are capable of affecting the catalytic ability of the porous materials. Knowing the surface area and porosity of the material helps to understand the structure and its potential applications in catalyzing reactions.

TGA is an analytical technique used to determine the thermal stability of material. The TGA patterns help to determine the fractions of volatile material present in the compound by monitoring the molecular weight of the compound as a function of temperature.

Characterization of Sn(IV) phenylphosphonates

$Sn(IV)(PhPO_3)_2$; H_2O, with HF

Figure 3 shows the XRD pattern of $Sn(IV)(PhPO_3)_2$; H_2O, with HF. The first sharp peak of 15.46Å corresponds to the interlayer d spacing of the material.

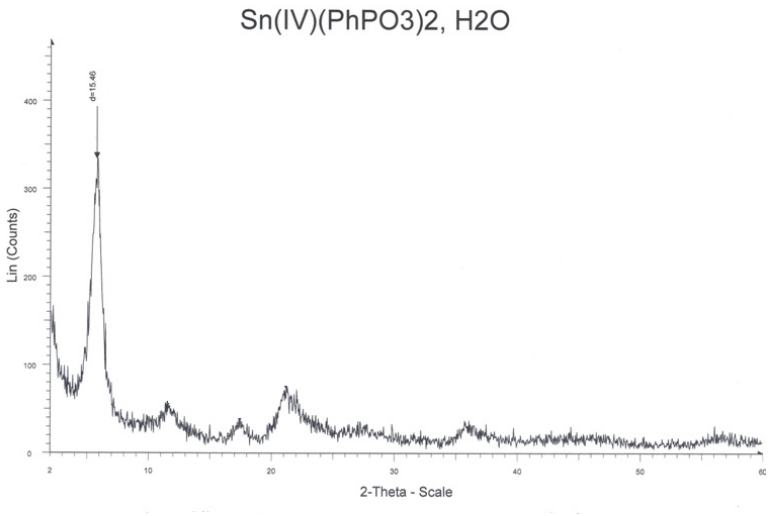

Figure 3. XRD pattern showing the d-spacing between layers of the SnPP synthesized in H_2O.

Figure 4 shows the N_2 sorption isotherm for $Sn(IV)(PhPO_3)_2$; H_2O.

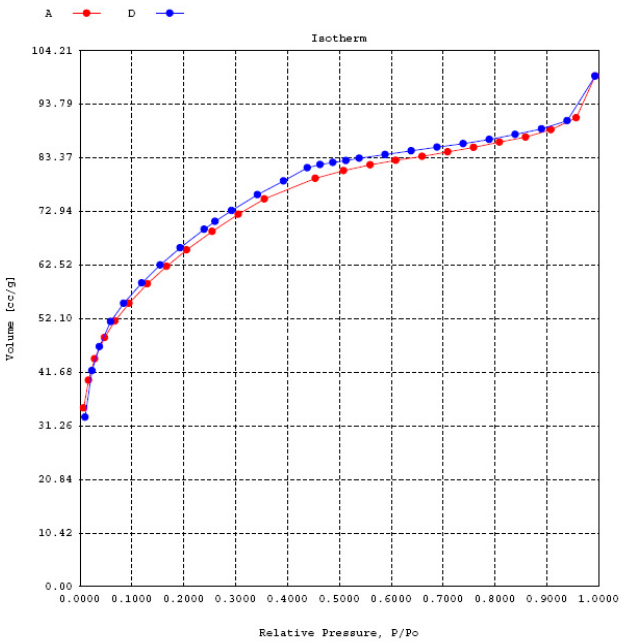

Figure 4. N_2 sorption isotherm of Sn(IV) phenylphosphonate synthesized in H_2O.

According to the analysis the following area-volume-pore size were calculated.

Surface area : 234 m^2/g

Total pore volume : 0.141cc/g

Average pore diameter : 24.1 Å

Figure 5 shows the Thermo Gravimetric Analysis data for the $Sn(IV)(PhPO_3)_2$; H_2O, with HF.

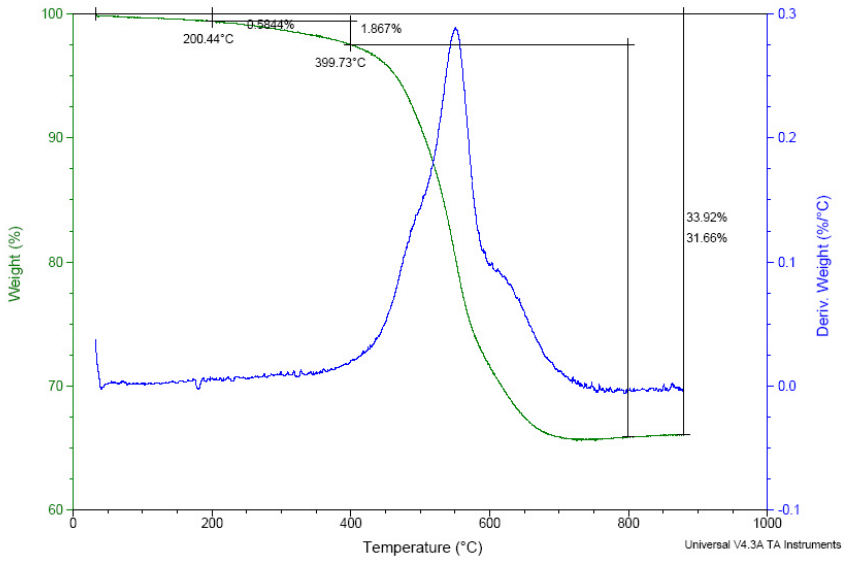

Figure 5. TGA data for Sn(IV) phenylphosphonate synthesized in H_2O.

When the TGA for $Sn(IV)(PhPO_3)_2$; H_2O, with HF (Figure 5) is considered, a total weight loss of 33.92% is observed at the end of the analysis. The following calculation shows molecular weights of the thermally dissociated material at each dissociation stage and the predicted chemical compositions.

Molecular weight of $Sn(O_3PC_6H_5)_2$. x H_2O. y HF	= 431 g/mol + (x*18+ y*20) g/mol
Total loss of HF and water (between 0 to 400^oC)	= 1.867% + 0.5844%
	= 2.4514%
Molecular formula before thermal dissociation	= $Sn(O_3PC_6H_5)_2$ *0.5 H_2O*0.1 HF
Molecular weight	= 442 g/mol
Molecular weight after loss of water	= 431 g/mol
Corresponding compound	= $Sn(O_3PC_6H_5)_2$
Total weight loss (between 0 to 800^oC)	= 33.92%
Remaining weight as a percentage	= 66.08%
Molecular weight of remaining compound	= 442 g/mol * 66.08%
	= 292 g/mol
Remaining material after complete dissociation	= SnP_2O_7

Using the TGA data the amounts of surface H_2O and HF in the material can be estimated and the remaining material after complete thermal dissociation can be predicted.

Sn(IV)($PhPO_3$)$_2$; EtOH, with HF

Figure 6 shows the XRD pattern of Sn(IV)($PhPO_3$)$_2$; EtOH, with HF. The first sharp peak of 15.34Å corresponds to the interlayer d spacing of the material.

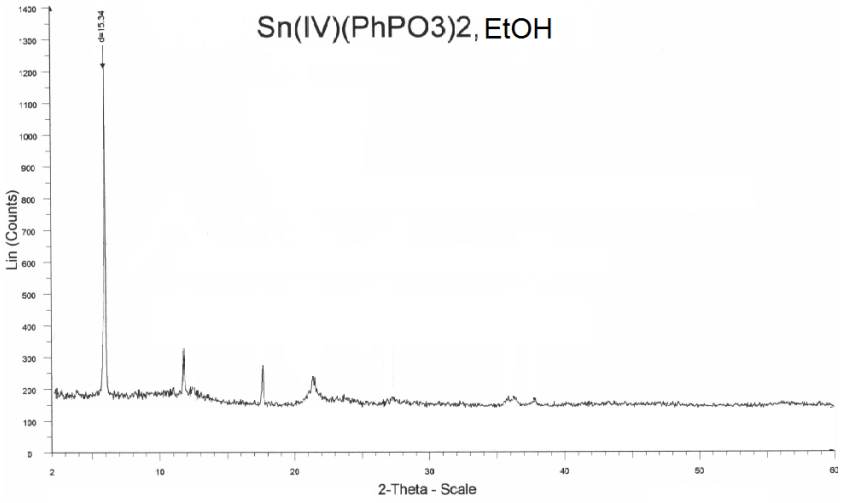

Figure 6. XRD pattern showing the d-spacing between layers of the SnPP synthesized in EtOH.

Figure 7 shows the N_2 sorption isotherm for $Sn(IV)(PhPO_3)_2$; EtOH.

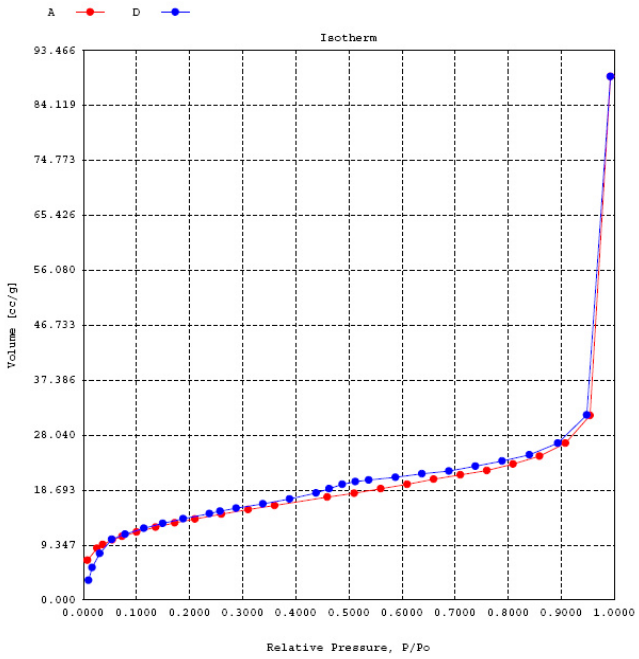

Figure 7. N_2 sorption isotherm of Sn(IV) phenylphosphonate synthesized in EtOH.

When compared to the isotherm of $Sn(IV)(PhPO_3)_2$ synthesized in H_2O, a low pore volume is observed for $Sn(IV)(PhPO_3)_2$ synthesized in EtOH. This may be due to incomplete closing of the pores during the analysis.

According to the analysis the following area-volume-pore size were calculated.

Surface area	:	49.2 m^2/g
Total pore volume	:	0.0486 cc/g
Average pore diameter	:	39.5 Å

Figure 8 shows the Thermo Gravimetric Analysis data for the $Sn(IV)(PhPO_3)_2$; EtOH.

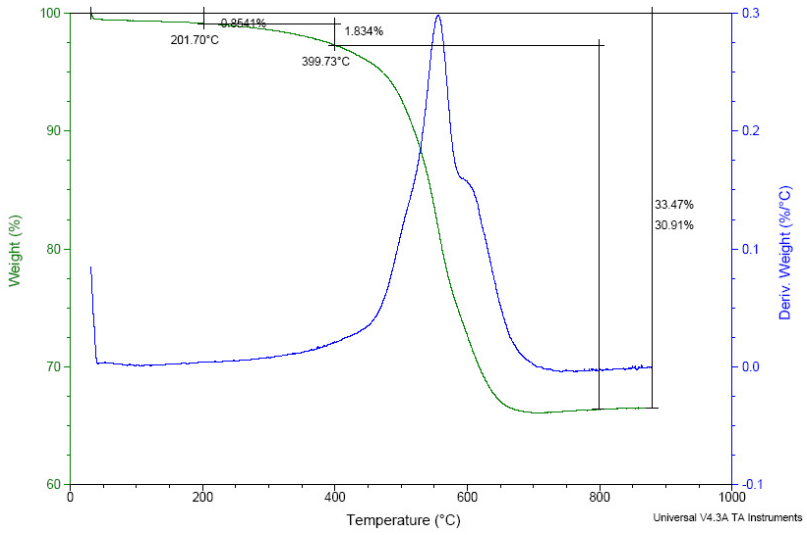

Figure 8. TGA data for Sn(IV) phenylphosphonate synthesized in EtOH.

Sn(IV)(PhPO$_3$)$_2$; DMSO, with HF

Figure 9 shows the XRD pattern of Sn(IV)(PhPO$_3$)$_2$; DMSO, with HF. The first sharp peak of 15.34Å corresponds to the interlayer d spacing of the material.

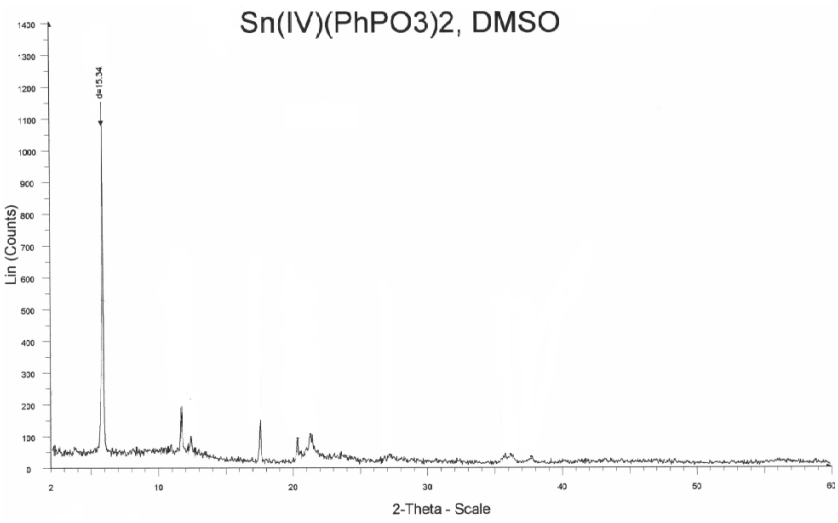

Figure 9. XRD pattern showing the d-spacing between layers of the SnPP synthesized in DMSO.

Figure 10 shows the N_2 sorption isotherm for Sn(IV)(PhPO$_3$)$_2$; DMSO, with HF.

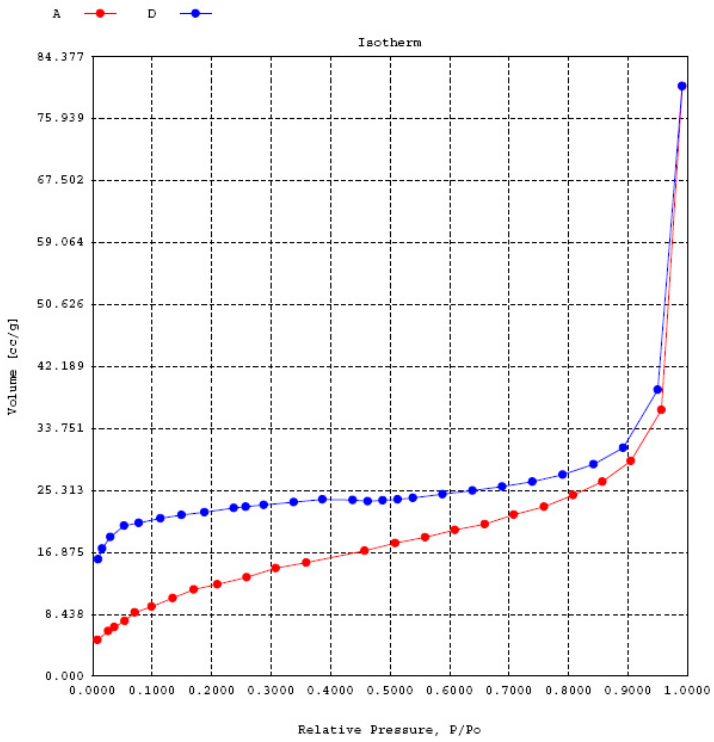

Figure 10. N_2 sorption isotherm of Sn(IV) phenylphosphonate synthesized in DMSO.

When compared to the $Sn(IV)(PhPO_3)_2$ synthesized in H_2O, the same material synthesized in DMSO shows a relatively low pore volume.

The following area-volume-pore size were calculated following the analysis.

Surface area	:	48.0 m^2/g
Total pore volume	:	0.0561 cc/g
Average pore diameter	:	46.7 Å

Figure 11 shows the Thermo Gravimetric Analysis data for the $Sn(IV)(PhPO_3)_2$; DMSO, with HF.

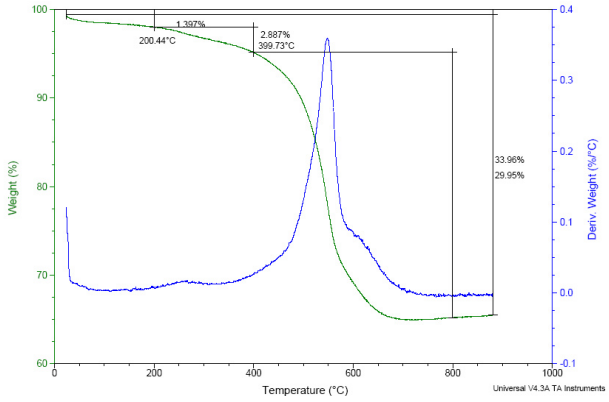

Figure 11. TGA data for Sn(IV) phenylphosphonate synthesized in DMSO.

$Sn(IV)Ph_2P_2$- HP; without HF; in DMSO and H_2O

Figure 12 shows the XRD pattern of $Sn(IV)Ph_2P_2$ - HP, without HF.

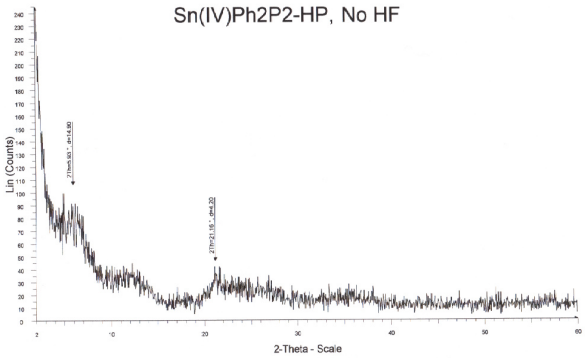

Figure 12. XRD pattern showing the d-spacing between layers of the SnPP-HP without HF.

Figure 13 shows the N_2 sorption isotherm for Sn(IV)Ph_2P_2-HP; without HF.

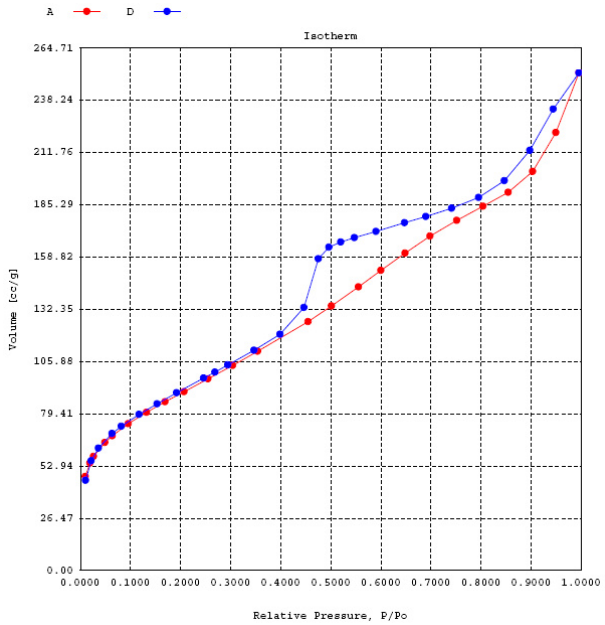

Figure 13. N_2 sorption isotherm of Sn(IV)Ph_2P_2-HP-without HF.

The shape of the curve (type IV) suggests that the material is mesoporous. According to the analysis the following area-volume-pore size were calculated.

Surface area	:	324 m^2/g
Total pore volume	:	0.343 cc/g
Average pore diameter	:	42.3 Å

Figure 14 shows the Thermo Gravimetric Analysis data for the Sn(IV)Ph_2P_2-HP, without HF.

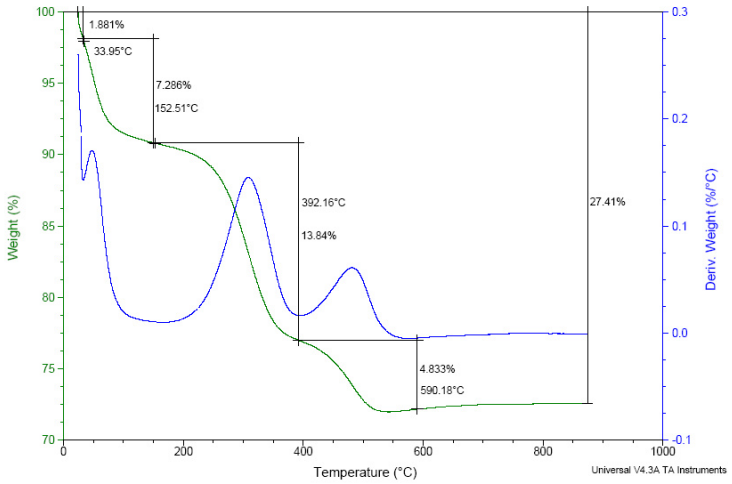

Figure 14. TGA data for Sn(IV)Ph_2P_2-HP-without HF.

Sn(IV)Ph_2P_2- HP; with HF; in DMSO and H_2O

Figure 15 shows the XRD pattern of Sn(IV)Ph_2P_2- HP; with HF.

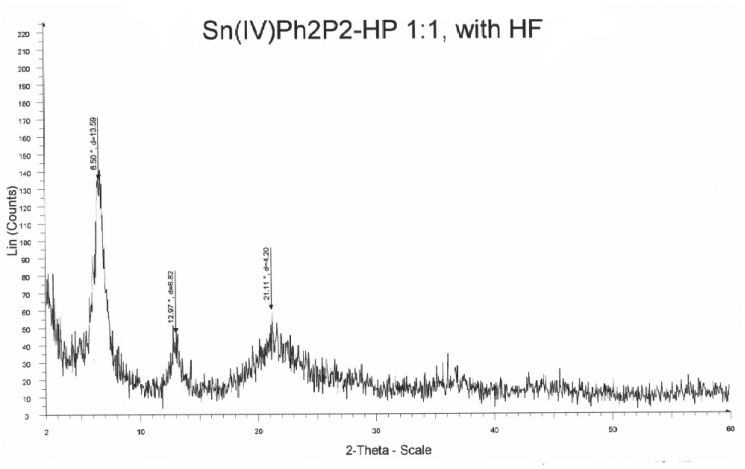

Figure 15. XRD pattern showing the d-spacing between layers of the SnPP –HP with HF.

Figure 16 shows the N_2 sorption isotherm for Sn(IV)Ph_2P_2-HP; with HF.

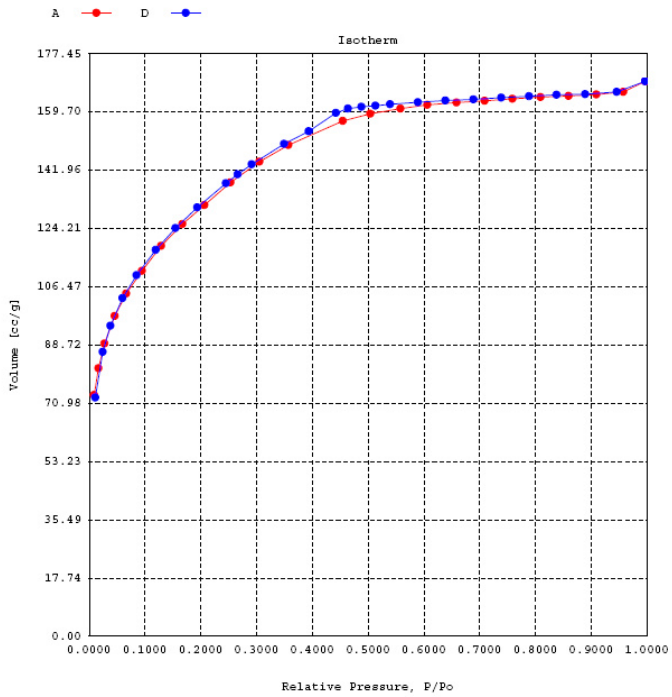

Figure 16. N_2 sorption isotherm of Sn(IV)Ph_2P_2-HP with HF.

The following area-volume-pore size were calculated using the analysis.

Surface area	:	468 m^2/g
Total pore volume	:	0.256 cc/g
Average pore diameter	:	21.9 Å

Figure 17 shows the Thermo Gravimetric Analysis data for the Sn(IV)Ph_2P_2-HP, with HF.

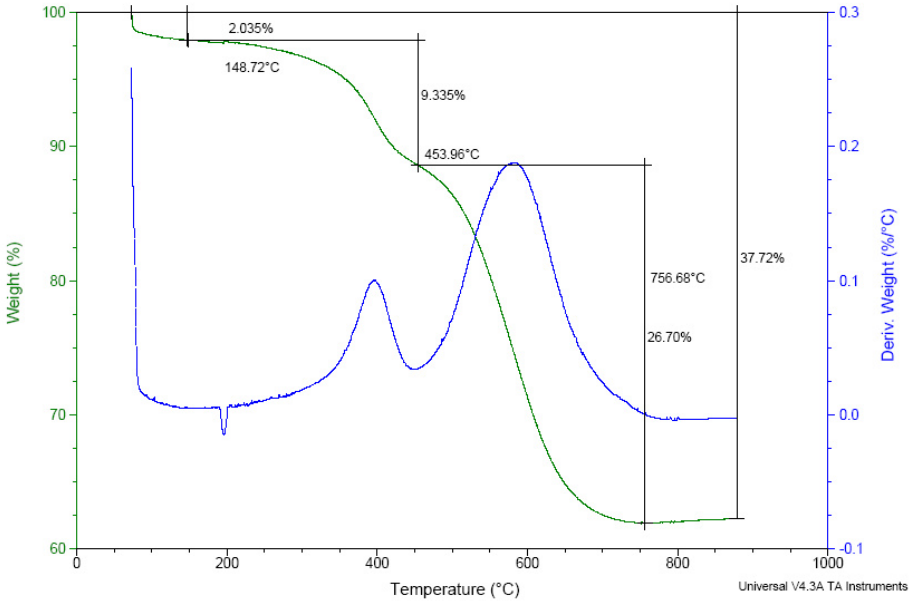

Figure 17. TGA data for Sn(IV Ph_2P_2-HP with HF.

When the TGA dissociation patterns of both Sn(IV) Ph_2P_2-HP with HF and without HF are analyzed, a complicated set of thermal dissociation patterns was observed. It is difficult to predict the structures of the decomposed material at each stage without x-ray patterns that correspond to each decomposition stage.

Characterization of mixed Sn(IV) phosphonates

$SnCl_4.5H_2O$: $PhPO_3H_2$: H_3PO_3 (3:4:2) – with HF; in DMSO and H_2O

Figure 18 shows the N_2 sorption isotherm for $SnCl_4.5H_2O$: $PhPO_3H_2$: H_3PO_3 (3:4:2) – with HF.

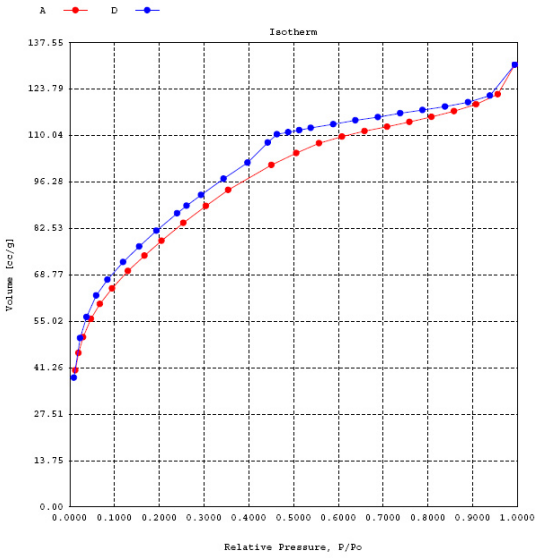

Figure 18. N_2 sorption isotherm of $SnCl_4.5H_2O$: $PhPO_3H_2$: H_3PO_3 (3:4:2) – with HF.

Using the analysis the following area-volume-pore size were calculated.

Surface area	:	285 m^2/g
Total pore volume	:	0.189 cc/g
Average pore diameter	:	26.6 Å

Figure 19 shows the Thermo Gravimetric Analysis data for $SnCl_4.5H_2O$: $PhPO_3H_2$: H_3PO_3 (3:4:2) – with HF.

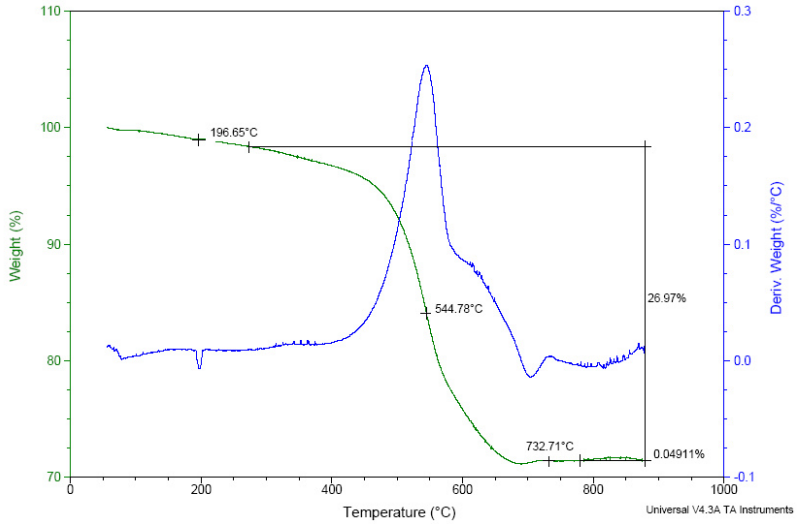

Figure 19. TGA data for $SnCl_4.5H_2O$: $PhPO_3H_2$: H_3PO_3 (3:4:2) – with HF.

$SnCl_4.5H_2O$: $PhPO_3H_2$: H_3PO_3 (3:4:2) – without HF

Figure 20 shows the N_2 sorption isotherm for $SnCl_4.5H_2O$: $PhPO_3H_2$: H_3PO_3 (3:4:2) – without HF.

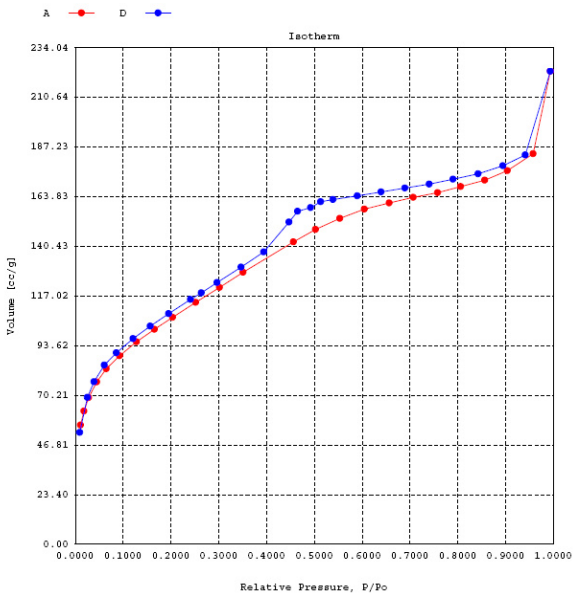

Figure 20. N_2 sorption isotherm of $SnCl_4.5H_2O$: $PhPO_3H_2$: H_3PO_3 (3:4:2) – without HF.

According to the analysis the following area-volume-pore size were calculated.

Surface area	:	385 m^2/g
Total pore volume	:	0.285 cc/g
Average pore diameter	:	29.6 Å

Figure 21 shows the Thermo Gravimetric Analysis data for $SnCl_4.5H_2O$: $PhPO_3H_2$: H_3PO_3 (3:4:2) – without HF.

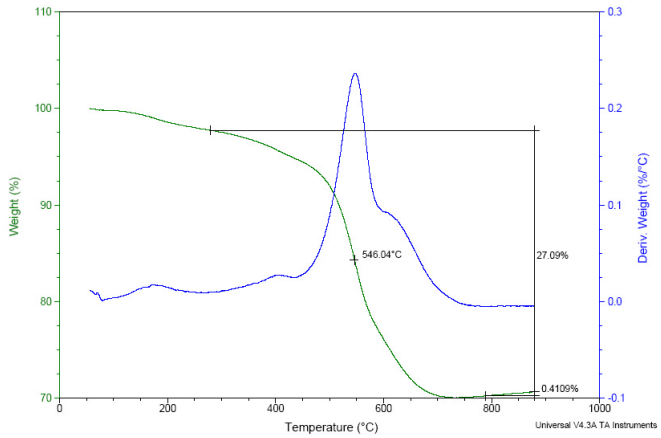

Figure 21. TGA data for $SnCl_4.5H_2O$: $PhPO_3H_2$: H_3PO_3 (3:4:2) – without HF.

$SnCl_4.5H_2O$: $PhPO_3H_2$: H_3PO_3 (1:1:1) – with HF; in DMSO and H_2O

Figure 22 shows the N_2 sorption isotherm for $SnCl_4.5H_2O$: $PhPO_3H_2$: H_3PO_3 (1:1:1) – with HF.

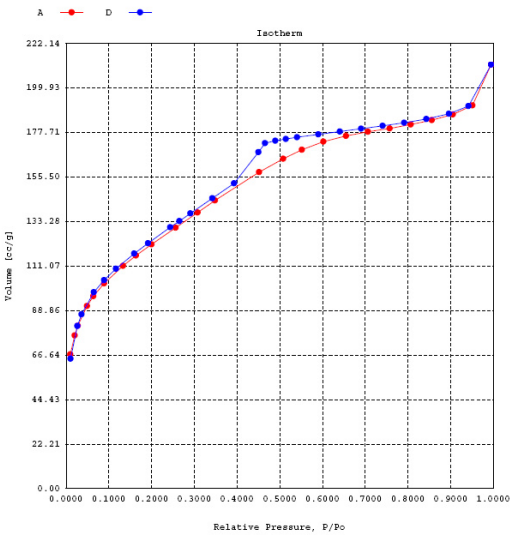

Figure 22. N_2 sorption isotherm of $SnCl_4.5H_2O$: $PhPO_3H_2$: H_3PO_3 (1:1:1) – with HF.

According to the analysis the following area-volume-pore size were calculated.

Surface area	:	440 m^2/g
Total pore volume	:	0.296 cc/g
Average pore diameter	:	26.9 Å

Figure 23 shows the Thermo Gravimetric Analysis data for $SnCl_4.5H_2O$: $PhPO_3H_2$: H_3PO_3 (1:1:1) – with HF.

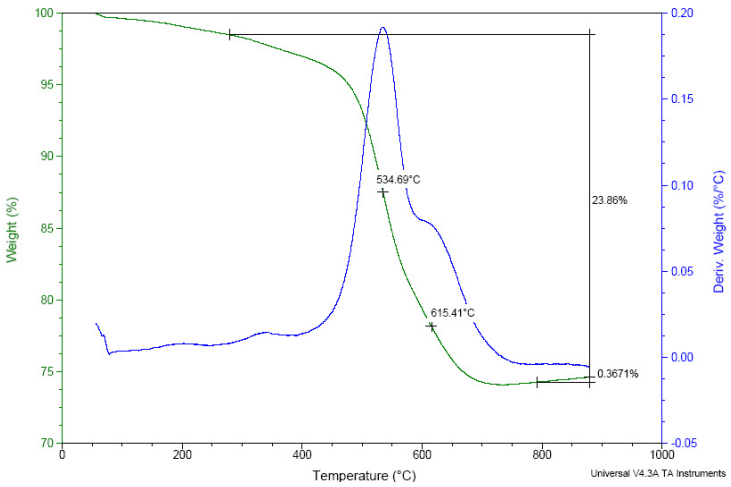

Figure 23. TGA data for $SnCl_4.5H_2O$: $PhPO_3H_2$: H_3PO_3 (1:1:1) – with HF.

$SnCl_4.5H_2O$: $PhPO_3H_2$: H_3PO_3 (1:1:1) – without HF; in DMSO and H_2O

Figure 24 shows the N_2 sorption isotherm for $SnCl_4.5H_2O$: $PhPO_3H_2$: H_3PO_3 (1:1:1) – without HF.

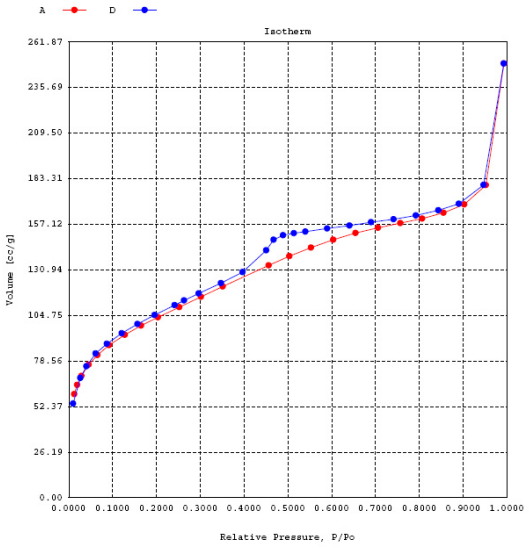

Figure 24. N_2 sorption isotherm of $SnCl_4.5H_2O$: $PhPO_3H_2$: H_3PO_3 (1:1:1) – without HF.

According to the analysis the following area-volume-pore size were calculated.

Surface area	:	372 m^2/g
Total pore volume	:	0.278 cc/g
Average pore diameter	:	29.9 Å

Figure 25 shows the Thermo Gravimetric Analysis data for $SnCl_4.5H_2O$: $PhPO_3H_2$: H_3PO_3 (1:1:1) – without HF.

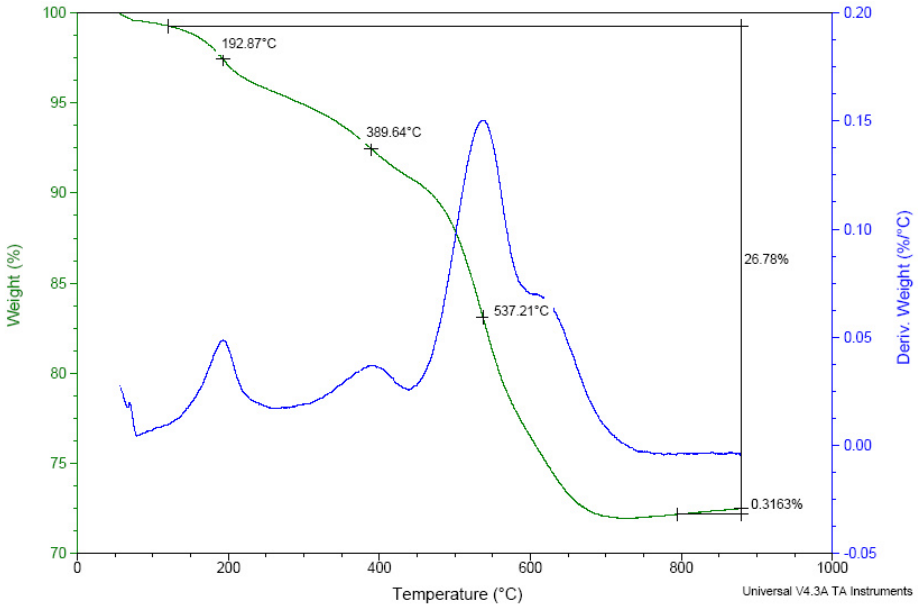

Figure 25. TGA data for $SnCl_4.5H_2O$: $PhPO_3H_2$: H_3PO_3 (1:1:1) – without HF.

When compared to the Sn(IV) $(PhPO_3)_2$, the mixed Sn(IV) phosphonates possess significantly high surface areas and total pore volumes. The TGA data for mixed Sn(IV) phosphonates show a lower total weight loss (~25%) during thermal decomposition than unmixed Sn(IV) $(PhPO_3)_2$ (~35%).

Study of the catalytic effects over Baeyer-Villiger oxidation

Study of the Presence of a Catalyst

Figure 26 shows a comparison between the percent conversion of para-ethoxy benzaldehyde with and without the catalyst. While 100% selectivity was observed for both reactions, when the aldehyde conversions are compared, a high conversion over 50% was observed for the reaction that was carried out in the presence of a catalyst

where poor conversion below 10% was observed for the reaction carried out in the absence of a catalyst.

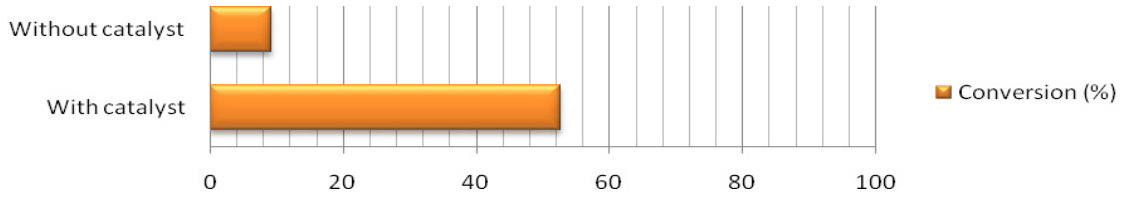

Figure 26. Percent conversion of para-ethoxy benzaldehyde (at 65 ^{o}C within 90 min) with and without $Sn(IV)(PhPO_3)_2;H_2O$.

Study of Weight of Catalyst

Figure 27 shows the percent conversion of the aldehyde and phenol selectivity of para-methoxy benzaldehyde with different amounts of catalyst.

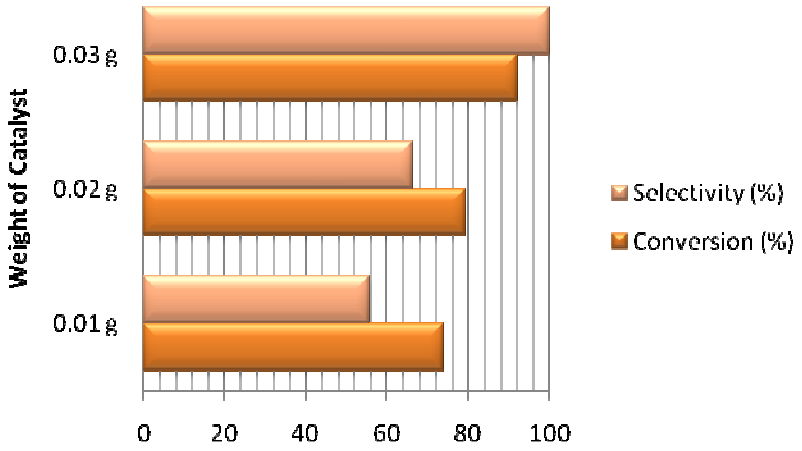

Figure 27. Percent conversion and selectivity of para-methoxy benzaldehyde (at 60 ^{o}C within 75 min) using different amounts of $Sn(IV)(PhPO_3)_2;H_2O$.

While 100% phenol selectivity was observed when 0.03 g of catalyst was used, a directly proportional relationship is apparent between aldehyde percent conversion and the amount of catalyst used in the reaction.

Study of Time

Figure 28 shows the percent conversion of para-methoxy benzaldehyde during different reaction periods.

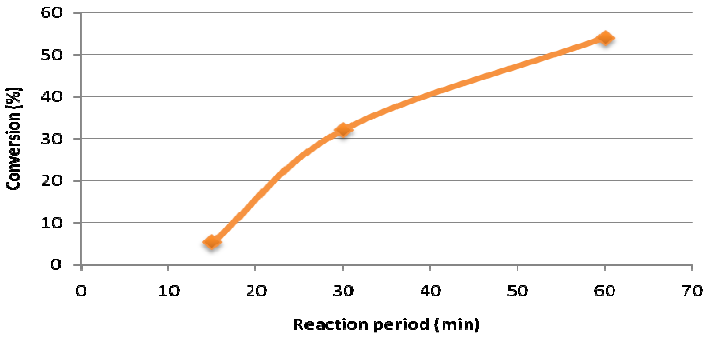

Figure 28. Percent conversion of para-methoxy benzaldehyde at 60 ^{o}C using Sn(IV)$(PhPO_3)_2$;H_2O at different reaction periods.

Although the aldehyde conversion increases with longer reaction periods, the conversion rate seems to decrease toward longer reaction periods.

Study of Catalytic Effect on Different Aromatic Aldehydes

Figure 29 shows the percent conversionand phenol selectivity of para-methoxy benzaldehyde and para-ethoxy benzaldehyde under same reaction conditions.

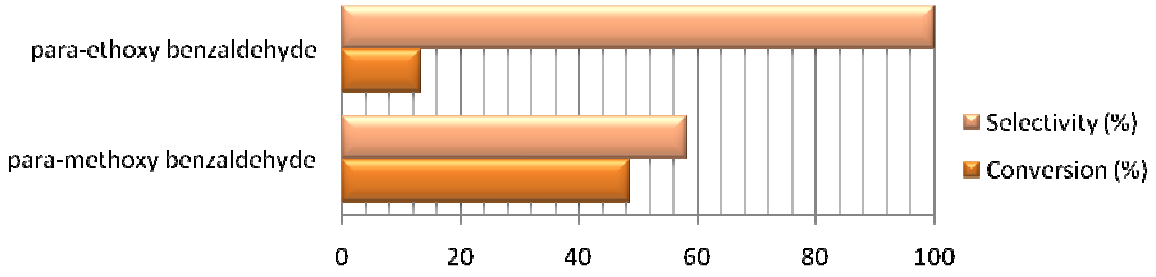

Figure 29. Percent conversion and selectivity of para-methoxy benzaldehyde and para-ethoxy benzaldehyde at 60 ^{o}C using Sn(IV)$(PhPO_3)_2$;EtOH for a reaction period of 60 min.

Although Sn(IV)$(PhPO_3)_2$;EtOH is more effective in converting para-methoxy benzaldehydes to its corresponding products, a 100% phenol selectivity was observed for the BV oxidation of para-methoxy benzaldehyde.

Figure 30 shows the percent conversion and phenol selectivity of para-methyl benzaldehyde and para-ethyl benzaldehyde under same reaction conditions.

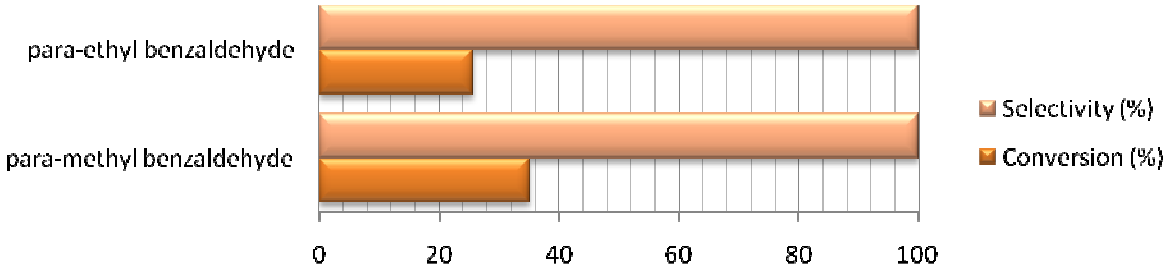

Figure 30. Percent conversion and selectivity of para-methyl benzaldehyde and para-ethyl benzaldehyde at 80 ^{o}C using Sn(IV)$(PhPO_3)_2$;EtOH for a reaction period of 180 min.

Similar to the previous study, Sn(IV)$(PhPO_3)_2$;EtOH is more effective in oxidizing para-methyl bezaldehyde than para-ethyl benzaldehyde. However, 100% phenol selectivity is observed for both reactions.

Study of the Effect of Different Catalysts on BV Oxidation

Figure 31 shows the percent conversion and phenol selectivity of para-methoxy benzaldehyde with three catalysts synthesized in different solvents.

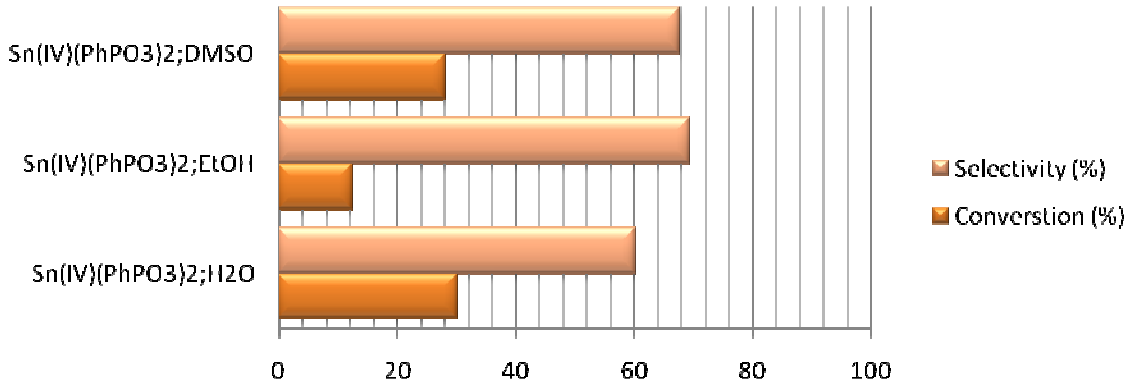

Figure 31. Percent conversion and selectivity of para-methoxy benzaldehyde at 50 ^{o}C for a reaction period of 60 min.

While Sn(IV)$(PhPO_3)_2$ synthesized in H_2O and DMSO show high aldehydes conversions, Sn(IV)$(PhPO_3)_2$ synthesized in EtOH shows a relatively low conversion of para-methoxy benzaldehyde. This may be explained in terms of the relatively low pore volumes observed for Sn(IV)$(PhPO_3)_2$;EtOH (Figure 7) when compared to Sn(IV)$(PhPO_3)_2$ in H_2O and DMSO. However, a relatively high phenol selectivity was

observed for $Sn(IV)(PhPO_3)_2$ synthesized in H_2O and EtOH than $Sn(IV)(PhPO_3)_2$ synthesized in DMSO.

Figure 32 shows the percent conversion and selectivity of para-ethyl benzaldehyde with two catalysts synthesized in different solvents.

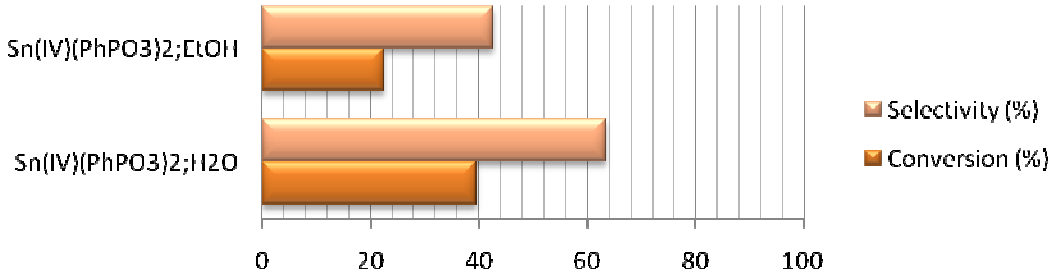

Figure 32. Percent conversion and selectivity of para-ethyl benzaldehyde to para-ethyl phenol at 80 ^{o}C for a reaction period of 180 min.

Similar consistency is observed for the two catalysts synthesized in H_2O and EtOH as the previous study where $Sn(IV)(PhPO_3)_2;H_2O$ shows a higher catalytic effect on conversion of para-ethyl benzaldehyde than $Sn(IV)(PhPO_3)_2$;EtOH. The same trend follows for the phenol selectivity of the reaction.

Figure 33 shows the percent conversion and phenol selectivity of para-ethyl benzaldehyde, para-methyl benzaldehyde and para-methoxy benzaldehyde with $Sn(IV)Ph_2P_2$ (1:1)-with HF.

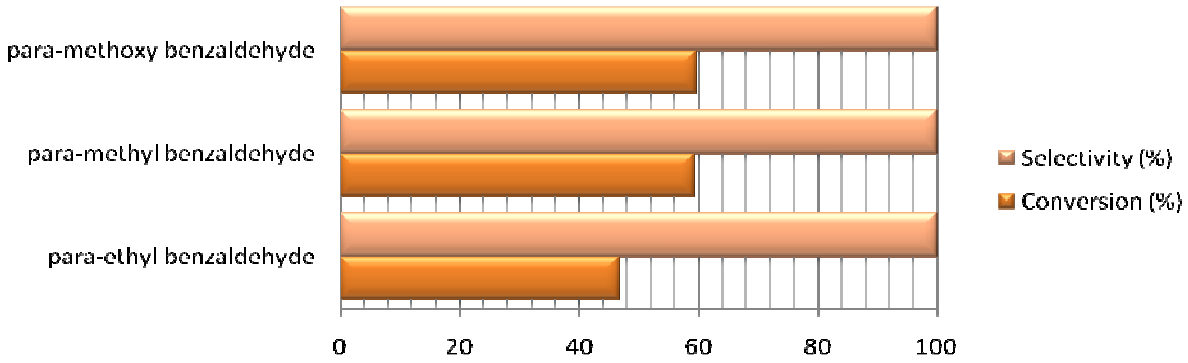

Figure 33. Percent conversion and selectivity of para-ethyl benzaldehyde, para-methyl benzaldehyde and para-methoxy benzaldehyde at 80 ^{o}C for a reaction period of 180 min.

At the presence of Sn(IV)Ph_2P_2 (1:1)-with HF, both para-methoxy benzaldehyde and para-methyl benzaldehyde show high conversions than para-ethyl benzaldehyde. However, 100% phenol selectivity was observed for all three aldehydes.

CHAPTER IV

SUMMARY AND CONCLUSIONS

The BV oxidation over 4-methoxybenzaldehyde carried out in the presence of different solvents using Sn(IV) phenylphosphonate (SnPP) as the catalyst showed that as the polarity of the solvent decreased the activity of the catalyst increased (Figure 34).

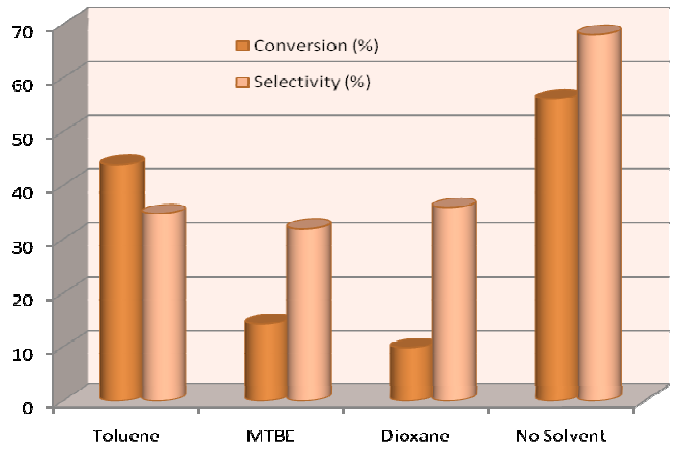

Figure 34. Effect of solvent on the BV reaction of para-methoxy benzaldehyde over SnPP catalyst; Reaction conditions: 60°C, 180 min, 3.7mmol of aldehyde and 4.5 mmol of 30% H_2O_2; 0.025g catalyst; 3 ml solvent.

This trend is opposite to what was observed over Sn-beta zeolites.[11] Amongst the different solvents used the conversion was the best for the least polar solvent toluene, which gave the aldehyde conversion of 42% and a selectivity to the phenol of 35%. The surprising result that we observed was that in the absence of a solvent the conversion

increased to 54% and the selectivity to the phenol increased to 68%. The hydrolysis of the ester to phenol is facile in the absence of a solvent. This result is extremely important in the BV oxidation as it eliminates the need to find a compatible solvent and also advances the cause of the environment as it eliminates the use for a solvent. We postulate that the SnPP materials being inorganic-organic hybrids are good hosts to both the organic reagents and H_2O_2, thus making them very active catalysts in this reaction. The interlayer d spacing of all three SnPP were around 15.3 Å (Figure 35).

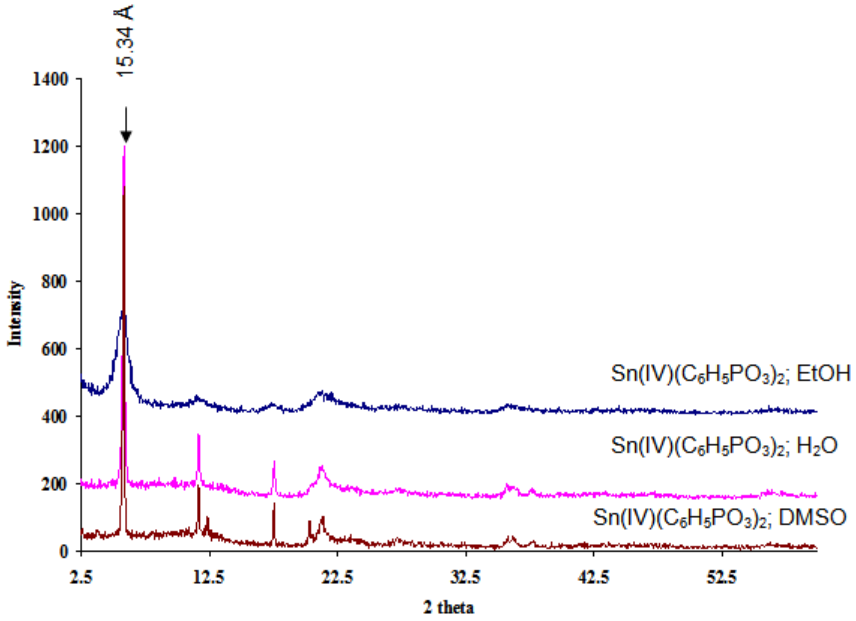

Figure 35. XRD patterns of SnPP materials synthesized in different solvents.

The effect of the catalyst characteristics on the reaction was studied by using a series of catalysts synthesized using different starting materials, mixed moalr ratios and different solvent systems. A summary of the results is shown in Table 1.

Table 1. Area-volume-pore size summary and BV oxidation of 4-methoxybenzaldehyde over different SnPP catalysts.

No	Catalyst	Surface area (m^2/g)	Total pore volume (cc/g)	Average pore diameter (Å)	Conversion (%)
A	$Sn(IV)(PhPO_3)_2$ in H_2O	234	0.141	24.1	30
B	$Sn(IV)(PhPO_3)_2$ in EtOH	49.2	0.0486	39.5	12
C	$Sn(IV)(PhPO_3)_2$ in DMSO	48.0	0.0561	46.7	28
D	$Sn(IV)Ph_2P_2$-HP; without HF in DSMO and H_2O	324	0.343	42.3	54
E	$Sn(IV)Ph_2P_2$-HP; with HF in DSMO and H_2O	468	0.256	21.9	58
F	$SnCl_4.5H_2O$: $PhPO_3H_2$:H_3PO_3 (3:4:2); with HF in DSMO and H_2O	285	0.189	26.6	24
G	$SnCl_4.5H_2O$: $PhPO_3H_2$:H_3PO_3 (3:4:2); without HF in DSMO and H_2O	385	0.285	29.6	19
H	$SnCl_4.5H_2O$: $PhPO_3H_2$:H_3PO_3 (1:1:1); with HF in DSMO and H_2O	440	0.296	26.9	29

Reaction coniditions: 50^oC, 1h, 3.7mmol of aldehyde and 4.5 mmol of H_2O_2 0.025 g catalyst

When the catalytic ability of $Sn(C_6H_5PO_3)_2$ synthesized in different solvent systems was compared, it was found that the catalyst made in DMSO and H_2O (A and C) were much more effective than the one synthesized in EtOH (A). When the aldehyde conversion of the mixed Sn(IV) phosphonates (F, G and H) is considered, the highest conversion is observed for the catalyst having a molar ratio 1:1:1 of $SnCl_4.5H_2O$:$PhPO_3H_2$:H_3PO_3 with

HF. The highest conversions are observed for catalysts D and E (Sn(IV)Ph_2P_2-HP with and without HF) and these catalysts also show relatively high surface areas.

When the surface areas and pore sizes of the catalysts are compared it is difficult to determine a direct relationship between the aldehydes conversions and the pore sizes. However, at slightly higher temperature of 65^oC, 100% conversion was observed within a reaction period of 3 hrs for all three $Sn(C_6H_5PO_3)_2$ synthesized in H_2O, EtOH and DMSO.

The catalysts were reused in the BV oxidation and it was found that there was no perceivable change in the activity of the catalyst. These catalysts show much higher catalytic activity compared to other heterogeneous catalysts reported in the literature (Table 2). The amount of Sn contained in our system is much higher than in the other Sn systems.

Table 2. Comparison of catalytic activity of different Sn catalysts with 4-methoxybenzaldehyde

Catalyst	Sn % weight	Conversion (%)	Selectivity (%)	Solvent comments
Beta Zeolite SnO_2	~2	56	46	Acetonitrile 50% H_2O_2 [10]
Sn Beta Zeolite	~2	79	79	Acetonitrile 50% H_2O_2 [9]
*Sn(IV)$(PhPO_3)_2$;H_2O	24.5	100	100	No solvent 30% H_2O_2

Reaction conditions: 80^oC, 7h, 3.7mmol of aldehyde and 4.5 mmol of H_2O_2: 0.05g catalyst (*0.025 g)

In conclusion, we have developed a new catalytic system whose surface area and pore size can be tailored and tuned over a wide range and these materials can catalyze the BV reaction under facile solvent-less condition to give conversion and selectivity levels higher than those reported in the literature so far.

REFERENCES

1. De Meijere, A. *Angew. Chem., Int. Ed.* **2005,** *44*, 7836-7840.

2. Ten Brink, G.-J.; Arends, I. W. C. E.; Sheldon, R. A. *Chem. Rev.* **2004**, *104*, 4105-4123.

3. Usui, Y.; Sato, K. *Green Chemistry* **2003**, *5*, 373-375.

4. Fischer, J.; Hoelderich, W. F. *Appl. Catal.A: Gen*. **1999**, *180*, 435-453.

5. Ueno, S.; Ebitani, K.; Ookubo, A.; Kaneda, K. *Appl. Surf. Sci.* **1997**, *121*, 366-371.

6. Kaneda, K.; Ueno, S.; Lmanaka, T. *J. Chem. Soc., Chem. Commun*. **1994**, 797-798.

7. Syper, L. *Synthesis* **1989**, *3*, 167-172.

8. Corma, A.; Navarro, M. T.; Nemeth, L.; Renz, M. *Chem. Commun.* **2001**, 2190-2191.

9. Corma, A.; Nemeth, L.T.; Renz, M.; Valencia, S. *Nature* **2001**, *412*, 423-425.

10. Renz, M.; Blasco, T.; Corma, A.; Fornés, V.; Jensen, R.; Nemeth, L. *Chem. Eur. J.* **2002**, *8*, 4708-4717.

11. Corma, A.; Fornés, V.; Iborra, S.; Mifsud, M.; Renz, M. *J. Catal.* **2004**, *221*, 67-76.

12. Huang, J.; Subbiah, A.; Pyle, D.; Rowland, A.; Smith, B.; Clearfield, A. *Chem. Mater.* **2006**, *18*, 5213-5222.

13. Subbiah, A.; Pyle, D.; Rowland, A.; Huang, J.; Narayanan, R. A.; Thiyagarajan P.; Zon J.; Clearfield A. *J. Am. Chem. Soc.* **2005**, *127*, 10826-10827.

CONTACT INFORMATION

Name:	Sandani Samarajeewa
Professional Address:	c/o Dr. Abraham Clearfield Department of Chemistry Texas A&M University College Station, TX 77843
Email Address:	sandani@tamu.edu
Education:	B.S. Chemistry, Texas A&M University, May 2008